

# Advances in Spacecraft Brine Water Recovery: Development of a Radial Vaned Capillary Drying Tray

Michael R. Callahan<sup>1</sup>, Miriam J. Sargusingh<sup>2</sup>, and Karen D. Pickering<sup>3</sup>  
NASA Johnson Space Center, Houston, TX, 77058

and

Mark M. Weislogel<sup>4</sup>  
Portland State University, Portland, OR, 97207

Technology improvements in the recovery of water from brine are critical to establishing closed-loop water recovery systems, enabling long—duration missions, and achieving a sustained human presence in space. A genre of ‘in-place drying’ brine water recovery concepts, collectively referred to herein as Brine Residual In-Containment, are under development. These brine water recovery concepts aim to increase the overall robustness and reliability of the brine recovery process by performing drying inside the container used for final disposal of the solid residual waste. Implementation of in-place drying techniques have been demonstrated for applications where gravity is present and phase separation occurs naturally by buoyancy—induced effects. In this work, a microgravity—compatible analogue of the gravity-driven phase separation process is considered by exploiting capillarity in the form of surface wetting, surface tension, and container geometry. The proposed design consists of a series of planar radial vanes aligned about a central slotted core. Preliminary testing of the fundamental geometry in a reduced gravity environment has shown the device to spontaneously fill and saturate rapidly, thereby creating a free surface from which evaporation and phase separation can occur similar to a terrestrial-like ‘cylindrical pool’ of fluid. Mathematical modeling and analysis of the design suggest predictable rates of filling and stability of fluid containment as a function of relevant system dimensions; e.g., number of vanes, vane length, width, and thickness. A description of the proposed capillary design solution is presented along with preliminary results from testing, modeling, and analysis of the system.

## Nomenclature

<i>ABS</i>	= acrylonitrile butadiene styrene
<i>Bo</i>	= bond number
<i>BRIC</i>	= Brine Residual In-Containment
<i>CAD</i>	= computer aided design
<i>DI</i>	= deionized
<i>ELS</i>	= exploration life support
<i>g</i>	= gravity
<i>IR</i>	= infrared
<i>ISS</i>	= International Space Station
<i>s</i>	= second
<i>SLA</i>	= stereolithography
<i>TS1</i>	= Test Solution #1

<sup>1</sup> Principal Investigator, Crew and Thermal Systems Division, 2101 NASA Parkway/EC3.

<sup>2</sup> Life Support Systems Engineer, Crew and Thermal Systems Division, 2101 NASA Parkway/EC2.

<sup>3</sup> Water Reclamation Technology Group Lead, Crew and Thermal Systems Division, 2101 NASA Parkway/EC3.

<sup>4</sup> Professor, Thermal and Fluid Sciences Group, Room 402m, Engineering Building, 1930 SW 4th Ave.

## I. Introduction

INCREASING water recovery has been identified as a major challenge in the NASA Technology Roadmap TA06, Human Health and Habitation Systems.<sup>1</sup> Closure of the water loop enables long-term operations both in microgravity and on planets. The water recovery goal set by the roadmap is 98-percent; this cannot be achieved without the recovery of water from wastewater brine. A significant challenge with achieving this level of recovery is associated with management of a multi-phase waste stream as brine transforms from a liquid, to a sludge, and finally to a wetted semi-/dried solid state. Additionally, the constituents of the waste water tend to be highly fouling to process hardware and toxic to crew.

A technique of “in-place” wastewater processing is being developed at the NASA. This technique involves processing waste water within the container used for final disposal of the solid brine residual. By processing the wastewater within its final disposal container, the need for complex waste transfer systems is obviated and opportunities for the waste products to come into contact with the crew are greatly reduced. The in-place drying technique is being applied to a genre of water recovery system concepts, collectively referred to herein as Brine Residual In-Containment (BRIC).

At the NASA Johnson Space Center, feasibility of in-containment drying technology was demonstrated for applications in which a gravity field was present, e.g. for a lunar or Martian habitat. The process is shown in Figure 1A. In this demonstration water was successfully evaporated from the brine into the gas phase and separated from the brine residual solid by buoyancy and/or forced convection.<sup>2</sup> Similarly, the brine residual was contained in the disposable liner within the evaporation container from which removal/disposal and replacement of the used liner was demonstrated.

In the absence of gravity, however, the process of containing the brine and maintaining an evaporative surface must be achieved by other means. Such separation may be achieved passively with wicks and semi-permeable membranes, Figure 1B, or actively by imparting a body force vector through rotation, Figure 1C.

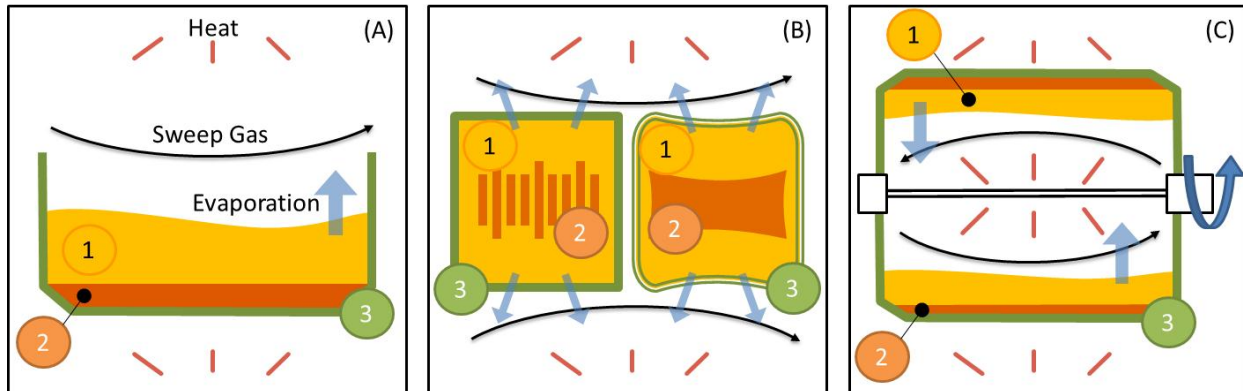


**Figure 1. BRIC concepts.** Figures highlight various means of phase separation for BRIC applications. (A) Solution buoyancy in a natural gravity field. (B) Uses surface force interaction for phase separation. (C) Uses solution buoyancy in an induced gravity field. Within each photo: (1) brine pool, (2) brine residual, and (3) the BRIC disposable element.

Static phase separation is an attractive approach for exploration missions due to the higher reliability and robustness generally offered by systems with no moving parts. Other BRIC-type technologies are being developed that make use of passive phase separation using, for example, permeable membranes and wicking technologies.<sup>3,4,5</sup>

The focus of the work presented in this paper was the development of a static phase capillary separation device that could maintain a free evaporative surface in microgravity; i.e. a ‘microgravity bucket’ or drying tray. Preliminary development focused on establishing a device geometry that would be expected to: (1) provide sufficient free surface area for unimpeded brine evaporation, (2) maintain stability of the brine pool when subjected to relevant loads, and (3) be capable of passive capillary pumping to fully saturate the device and maintain infilling rates during the dewatering process. A subscale model of the design was built and tested to prove that the fundamental aspects of the microgravity bucket would behave as theorized and to verify computational modeling to be used in future design work.

## II. Microgravity Container Design Concept

For the microgravity bucket concept capillary forces are generated using a combination of container geometry and surface tension forces. For this application, the capillary base unit is a wedge shape arranged in a radial tray format, Figure 2A. The tray contains the cylindrical brine pool within a drying chamber. As with the 1g static container concept, water is recovered from clean water vapor evaporating from the free surface while leaving waste brine solids behind. At the end of the process the mostly solid brine residual remains contained in the device which can then be disposed of, Figure 2B.

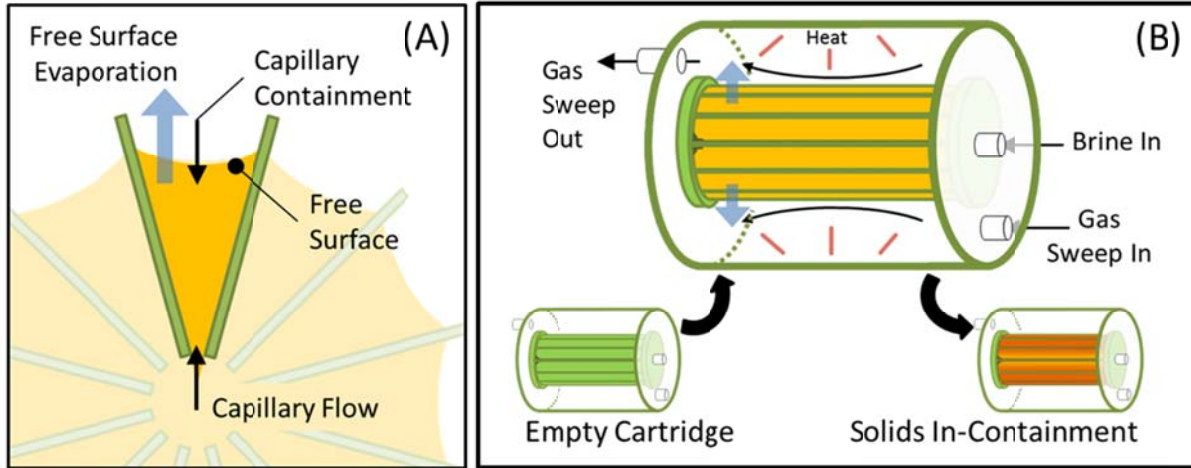


**Figure 2. Capillary based static containment BRIC concept.** Figure presents the concept discussed in this paper where (A) a wedge capillary device contains brine pool. Brine pool concentrates as water is evaporated and removed by the sweep gas. The remaining brine residual (B) may be discarded with the capillary device.

### A. Wedge Corner Angle

As described above, the base geometric unit of the capillary drying tray is a wedge corner angle formed by to vanes on intersecting planes. The capillary fluidics of the wedge corner angle is described in Thomas et al.<sup>6</sup> and Weislogel et al.<sup>7</sup>, and summarized in Figure 3. According to capillary theory,  $\alpha$  is the half angle of the wedge,  $\theta$  is the contact angle of the fluid on the wedge material,  $R$  is the principal radius of curvature of the fluid meniscus,  $h$  is the height of the liquid within the wedge, and  $P_\alpha$  and  $P_2$  describe the capillary underpressure, i.e. the pressure rise across the liquid free surface.

The wedge corner angle is constrained by the Concus-Finn<sup>8</sup> critical corner wetting condition defined in Eq. (1), and the capillary underpressure in the liquid defined in Eq. (2), where  $\sigma$  is the surface tension of the liquid.

$$\alpha \leq 90 - \theta \quad (1)$$

$$P_\alpha - P_1 = \frac{-\sigma}{R} = \frac{-\sigma}{h} \left( \frac{\cos \theta}{\sin \alpha} - 1 \right) \quad (2)$$

The corner angle selected for this work was based on a worst-case wetting of brine on a substrate of polypropylene, determined to be approximately  $\theta = 82.5^\circ$  (data not shown). The resulting half-angle  $\alpha$  from Eq. (1) is therefore less than or equal to  $7.5^\circ$ , i.e., the corner angle for each containment wedge should be no more than  $15^\circ$ . The preliminary capillary conduit cross-section, therefore, assumed a 24 vane,  $15^\circ$  angle configuration.

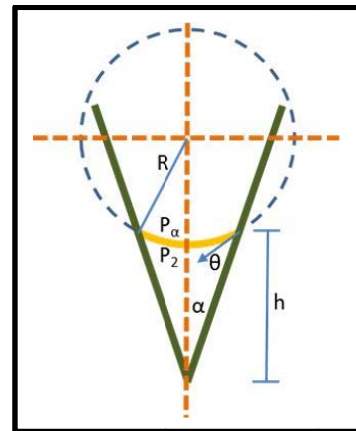


**Figure 3. Sectional schematic of liquid configuration in a wedge with notation adopted.**

## B. Free Surface Area

A driving requirement for BRIC capillary device is that it provides sufficient evaporation at the free surface over the outer opening of each vane. A maximum brine processing rate for an exploration mission of 4kg/day with a 20-hr duty cycle was assumed. The evaporative flux was estimated at  $1.05 \times 10^{-4}$  kg/hr-cm<sup>2</sup> based on previous testing of the 1-g static BRIC system. To provide sufficient evaporation of the drying cycle the capillary conduit would need to provide approximately 1900 cm<sup>2</sup> of surface area.

## C. Microgravity Container Design

The concept for a passive microgravity brine evaporation container is shown in Figure 2. Again, the design is derived using a series of capillary wedge units, as described above. The wedges arranged about a center axis are made to form a cylindrical shape which reduces the footprint of the device and provides a common port for filling. The length and diameter of the device was selected to meet the required free surface area for evaporation, resulting in a basic cylindrical geometry with a diameter of 16.5 cm (6.5 in.) and a length of 38.1 cm (15 in.). The core of the cylinder is bored through the center axis, removing some portion of the interior corner angle of each wedge and forming a slitted passage running the length of the structure. Caps on either end of the cylindrical structure provide containment of the fluid with a hole of slightly larger diameter than the central core serving as a port for filling the device. In total, the container geometry provides for rapid and spontaneous filling, distribution, and containment of liquid while supplying a free surface area from which evaporation can occur over the open face of the cylindrical device.

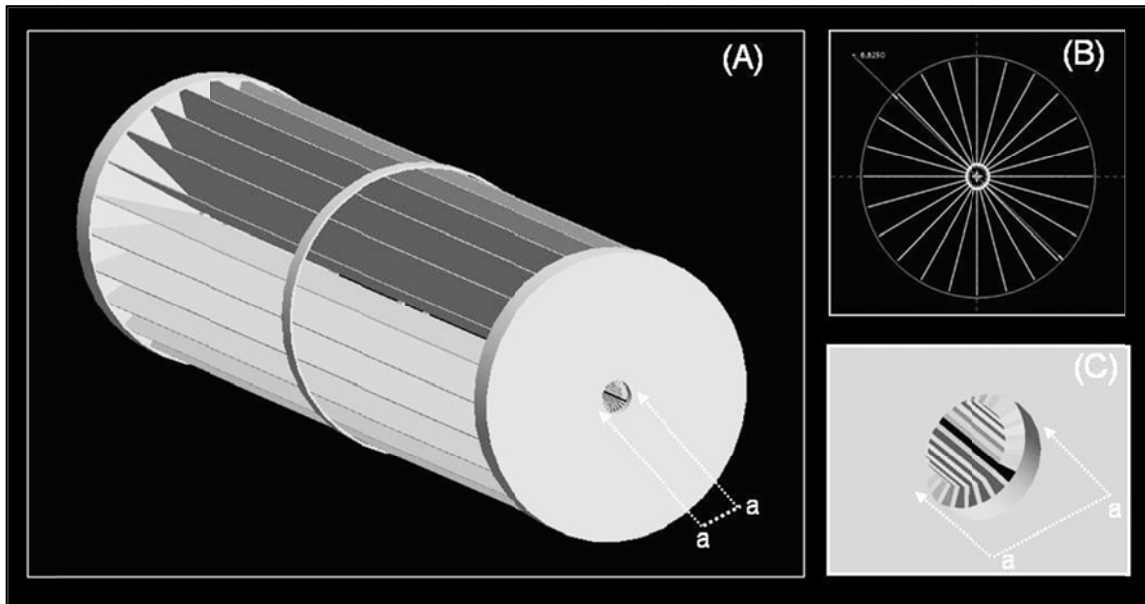


**Figure 3. Graphic of a concept for a BRIC static microgravity fluid container. (A) Graphic of the BRIC Radial Vaned Capillary Drying Tray; (B) A cross-section; (C) close-up of the center fill port showing cross-communication of interior corner vanes**

## III. Analysis and Test

With a basic geometric concept derived, it is possible to begin some preliminary analysis and test of the device. Two performance areas of initial interest were establishing estimates of the container's stability and flow characteristics. In this work, capillary stability against forces imparted axially and longitudinally on the wedge structure were considered. Other forces that may disrupt stability of the fluid in the container, such as shear forces imparted by a sweep gas, will need to be evaluated in future design analysis. Similarly, the characterization of fluid flow within the device was limited to the initial fill of the structure and the derived flow during continuous filling of the device as water is removed during the drying process. Further evaluation on the effects of solids accumulation on the passive infill process also is needed, as well as, an integrated demonstration of the capillary fluidics over the full brine drying process.

## A. Capillary Stability Assessment

### Methods for Stability Assessment

For the capillary drying tray to work in microgravity it must ultimately be stable both at rest and when subjected to spurious forces that may otherwise destabilize the gas/liquid/solid interface. Stability of fluids within a wedge can be defined as the effective dominance of surface tension forces relative to body forces that may be imparted on tray that might otherwise “spill” the container. The stability of the device may be characterized with high confidence via critical bond number relationships.<sup>9</sup> Eq. (3) provides the general bond number equation, where  $\rho$  is the density difference across the free surface,  $a$  is the applied force, and  $L_c$  is a characteristic free surface length.

$$Bo = \frac{\rho \cdot a \cdot L_c^2}{\sigma} \quad (3)$$

The bond number  $Bo_1$  defined in Eq. (4) refers to the stability against forces applied axially across a cylinder where  $R$  is the radius of curvature or the approximate half width of the corner vane interface. Similarly, the bond number  $Bo_2$  defined in Eq. 5 refers to the stability against forces applied longitudinally along the unit's length,  $L$ .

$$Bo_1 = \frac{\rho \cdot a \cdot R^2}{\sigma} \quad (4)$$

$$Bo_2 = \frac{\rho \cdot a \cdot R \cdot L}{\sigma} \quad (5)$$

Typically, for circular cylindrical geometries, bond numbers above 3 are considered to be always unstable, numbers less than 0.8 are considered always stable, and numbers between 3 and 0.8 are potentially stable or unstable, depending on the relative magnitude of the competing forces. The method used to assess the capillary stability of the BRIC container was to set the bond numbers in Eq. (4) and Eq. (5) to a value of 3. The equation is then solved for  $a$ , the maximum force at which surfaces might be stable. The ratio of the threshold value,  $a$ , for stable surfaces to the destabilizing event was used to determine the factor of safety inherent in the design. For this design, it was desired that a factor of safety of at least 3 in each direction be achieved.

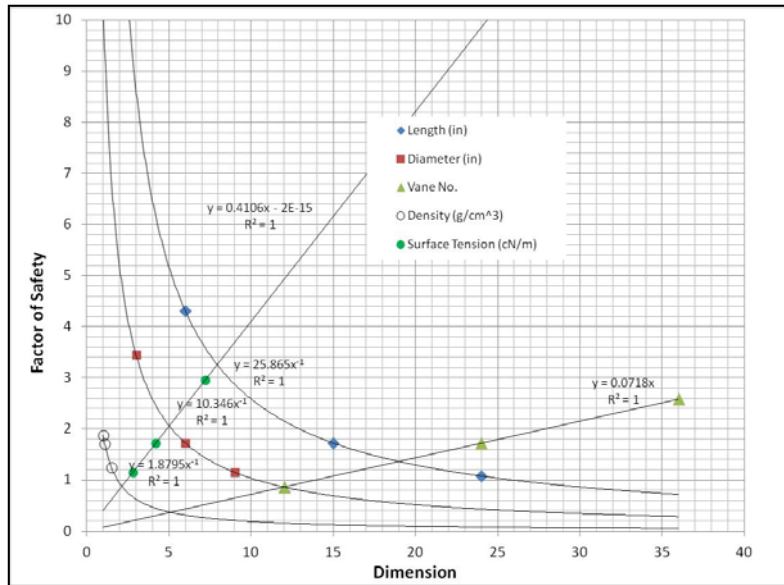


**Figure 4. Sensitivity Analysis on Raidal Vaned Capillary Stability.** Presents affects of cylinder length, diameter, vane density, and fluid design and surface tension on longitudinal stability ( $Bo_2$ ) versus an ISS reboost event.

The destabilizing force considered was a reboost of the International Space Station (ISS), estimated at  $1.8 \times 10^{-3} g$ . The preliminary dimensions for the BRIC capillary device were those previously described. The working fluid was assumed to be a brine generated from a wastewater solution comprised of pretreated urine and humidity condensate recovered to approximately 93.5%. A further description of the solution, referred to as Exploration Life Support Test Solution 1 (ELS TS1), can be found in McQuillan et. al.<sup>10</sup> For the stability analysis, the surface tension and density of the TS1 brine were estimated at 0.042 N/m and 1,090 kg/m<sup>3</sup> to 1200 kg/m<sup>3</sup>, respectively, based on previous measurement of the thermophysical properties of ELS TS1 and other brines (data not provided).

The destabilizing force considered was a reboost of the International Space Station (ISS), estimated at  $1.8 \times 10^{-3} g$ . The preliminary dimensions for the BRIC capillary device were those previously described. The working fluid was assumed to be a brine generated from a wastewater solution comprised of pretreated urine and humidity condensate recovered to approximately 93.5%. A further description of the solution, referred to as Exploration Life Support Test Solution 1 (ELS TS1), can be found in McQuillan et. al.<sup>10</sup> For the stability analysis, the surface tension and density of the TS1 brine were estimated at 0.042 N/m and 1,090 kg/m<sup>3</sup> to 1200 kg/m<sup>3</sup>, respectively, based on previous measurement of the thermophysical properties of ELS TS1 and other brines (data not provided).

### Results for Stability Assessment

The resultant factors of safety from determined from Eqs 4 and 5 were 66 in transaxial direction and slightly less than 2 in the longitudinal direction. Using this same model, a sensitivity analysis was performed to determine the effect of scaling dimensional parameters within the design, e.g., radius, length, vane number, density, and surface tension, on the safety factors ascribed to the  $\text{Bo}_2$  stability. The results are plotted in Figure 4. The data show that the combination of diameter, length, and vane number can be optimized to produce a more favorable stability profile. This analysis tool can be used in future design work in order to optimize the stability of the capillary containment device. However, the effects of such changes on the overall performance of the device, such as the amount of available evaporation area, will also need to be considered.

### B. Capillary Flow

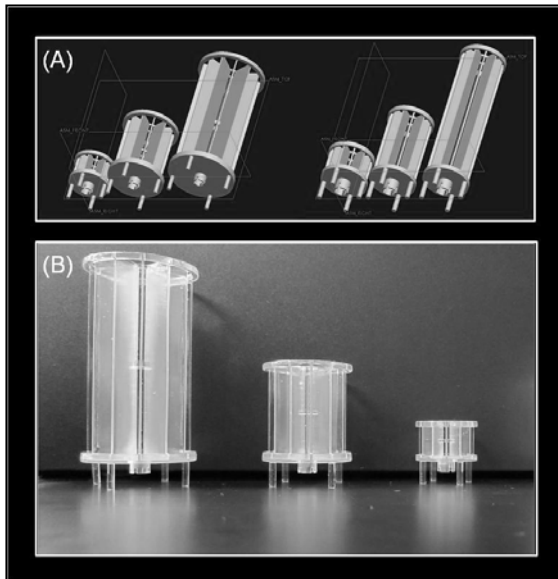


**Figure 5. Subscale Test Articles.** (A) CAD model of subscale radial vaned capillary tray test parts. (B) Physical test parts manufactured by stereolithography in clear, ABS-like material.

chamber which free falls over 22 m (2.13 s). The capillary devices were interfaced with a reservoir containing a test solution of highly wetting 0.65 centistoke silicon oil (manufactured by Dow Chemical). The test solution was selected for its low viscosity and high wetting properties, which allow for fast response times. Despite the difference in the thermophysical properties of oil and brine, predictions of flow

### Methods for Flow Assessment

In addition to stability, a preliminary assessment of the flow characteristics of the microgravity bucket was undertaken. Assessment of flow included the mechanics and rate of filling of the tray volume. To do this, a series of six subscale test articles were designed and built in a radial vane configuration approximating that of the full device. The test articles varied in both length and radius. Test part sizes were determined based on predictive models for capillary flow, the short times associated with drop-tower testing, and the physical constraints associated with manufacturing the subscale parts. The design allowed the test articles to be dropped in various orientations to capture the maximum flow rate achievable with the proposed the geometric design. Figure 5A illustrates some representative CAD models of the developed parts as well as examples of parts manufactured using stereolithography (SLA) techniques in clear acrylonitrile butadiene styrene (ABS) like materials, Figure 5B.

The test cells were dropped in the Dryden Drop Tower at Portland State University. Figure 5 shows a graphical representation of the drop tower and a schematic of the drop-tower experimental test rig. The test cells were released in an aerodynamically shielded

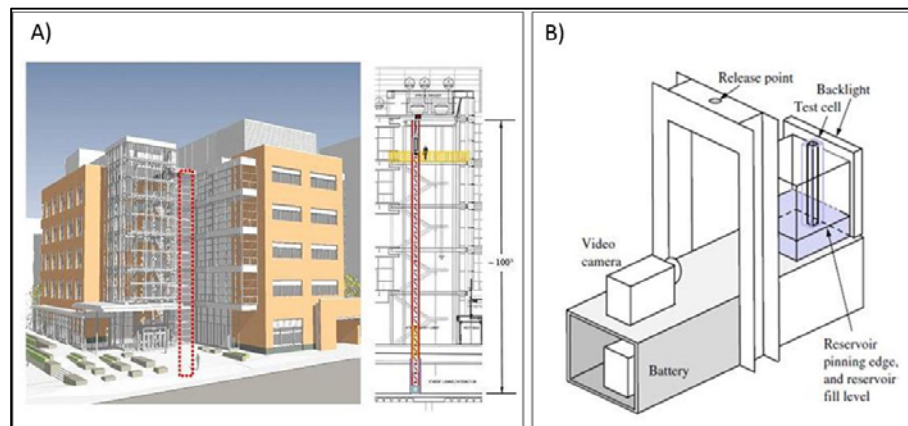


**Figure 6. Drop Tower Test Facility.** A) Graphical representation of Dryden Drop Tower at Portland State University reproduced with permission from <http://www.ddt.pdx.edu/node/599>; B) Schematic of simple drop-tower package.

behavior are expected to differ significantly only in time of response. These differences can be predicted once models are developed for the flow in the subscale devices. Preliminary work in modeling these flows was initiated by comparing drop-tower test data and models for predicting cylindrical and compound capillary flow.<sup>11</sup> The models cited in the paper are for bulk flow length in cylinders and for corner flow length and bulk flow associated with compound capillary rise. See Eqs. (2.6), (11.1), (11.2), and (11.3), respectively, in the Weislogel paper cited above.

*Results for Flow Assessment*

Figure 7 illustrates some of the BRIC subscale drop-tower testing performed. The figure shows a 3 cm x 5 cm test cell placed upright in a reservoir of 0.65 centistokes silicon oil. Notable elements include the rapid onset of capillary rise and capillary corner flow in both the center core and lower portion of the radial vanes after 0.14 seconds ( $t = 0.14$  s). Capillary rise continues with time, but the rise is dominated by the flow of the liquid up the center channel core until it reaches the end of the test cell by  $t = 0.5$  s. The liquid then “pins” on the upper edges of the test article; i.e., liquid does not move radially along the ceiling of the cell. Liquid pinning at the top of the test article is an artifact of the cell design. Signs of radial infill become evident as the liquid

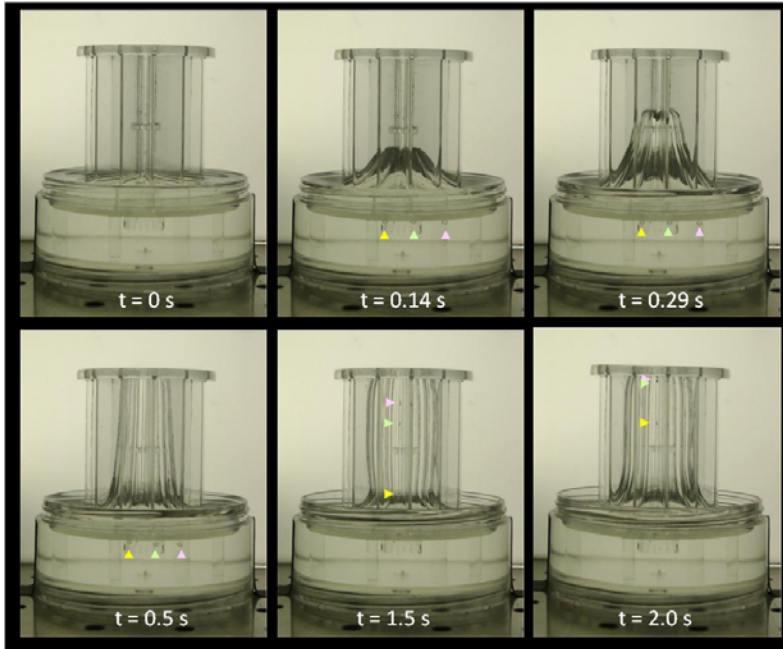


**Figure 7. Example of BRIC subscale drop-tower test**

boundary layer is observed to thicken outward through the 1.5 s and 2.0 s timeframes. Interestingly, radial filling appears to occur by the continuous flow past the pinning edges at the top of the device, and back down and out along the path of highest capillary pressure where multiple corner angles are formed at the interface between the vanes and the lower end cap. The fill mechanism can be partially observed in the still photos by the movement of three small bubbles observed first at  $t = 0.14$  s in the liquid reservoir near the inlet of the test cell. These bubbles are indicated by the yellow, green, and pink triangles in Figure 7. At  $t = 0.5$  s, the bubbles are pulled closer to the inlet port. At  $t = 1.5$  s, the pink and green bubbles are pulled into the center core flow and are about three-quarters of the way up the center channel. At  $t = 2.0$  s, the pink and green bubbles are pinned at the top of the cell, and the yellow bubble is observed to be about halfway up the center channel.

Analysis and modeling of the drop-tower test data is continuing. A preliminary assessment of flow of the inverted test cells was completed using the model describing compound capillary flow. The initial model predictions for compound capillary lengths and flow rate coefficients over predicted the experimental flow rates by 60 percent to 75 percent. Model agreement was improved by

adjusting the viscous resistance term,  $\phi$  ( $\phi$ ). The original model predictions for capillary length and flow are shown with the model-adjusted values provided in Table 3. The offset in the model predictions suggests that the geometry of the baseline BRIC container may exhibit a new theoretical regime for compound capillary flow. This finding is being further investigated and expected to be significant within the field of capillary fluidics.

**Table 1. Model Estimates of Compound Capillary Flow**

Physical Cell			Flow Velocity (cm/s)		Flow Coef.(mL/s <sup>1/2</sup> )	
Radius (cm)	Length (cm)	Volume (cm <sup>3</sup> )	Model Predicted	Model Adjusted	Model Predicted	Model Adjusted
2	2	10	6.8	2.7	22.8	9.1
3	5	48	11.2	4.5	69.1	27.7
4	10	157	25.1	10.0	248.0	99.2
15.2	38.1	7500	-	1.7	-	242.6

With the adjusted model, it is now possible to estimate the capillary flow for a full-scale BRIC containment device. These data are presented in Table 1 using the baseline scaling dimensions and the ELS TS1 brine. The data suggests that the velocity of flow is reduced to approximately 1.7 cm/s. At this flow rate, the expected time to complete filling of the internal volume of the BRIC container is estimated to be less than 15 seconds; a rate which is predicted to be 54 times faster than the rate of evaporation.

To provide early insight into the predicted behavior of the BRIC capillary device, the modeling data can be used to investigate which parameters might be changed to improve the flow dynamics of the evaporator design. These data are provided in Figure 8.

For this analysis, the baseline dimension of the proposed BRIC container design was again used unless specified within the figure key as a parameter of dimensional change. This early modeling shows that the length of the device has little effect on flow rate. When vane number is increased flow is observed to pass through a maximum that is limited by increasing the surface-area-to-volume ratio and, thereby, increasing the viscous resistance.

On the other hand, increasing the diameter increases flow as the square of the cross-sectional area, decreasing the surface-area-to-volume ratio and lowering viscous resistance. Since evaporation rates can be expected to reach limits associated with the brine depth and diffusion length over the vane height, increasing the system diameter may not be favorable. Finally, decreasing surface contact angle is shown to increase flow rates significantly.

The data suggest that selection of materials used to build the BRIC container should be considered an important parameter in the design. Limited testing to date has shown that specific surface treatments with hydrophilic materials on plastic can reduce surface contact angles for deionized (DI) water by more than 50 percent. Similarly, data collected for contact angles of DI water on polypropylene have shown decreases from nearly 100° on virgin plastic material to less than 10° for surfaces upon which brine material has been dried (data not shown). Other surfaces are also under consideration, focused on wetting materials that can be worked into collapsible designs that would minimize the up-mass and disposal volume used for a flight system.

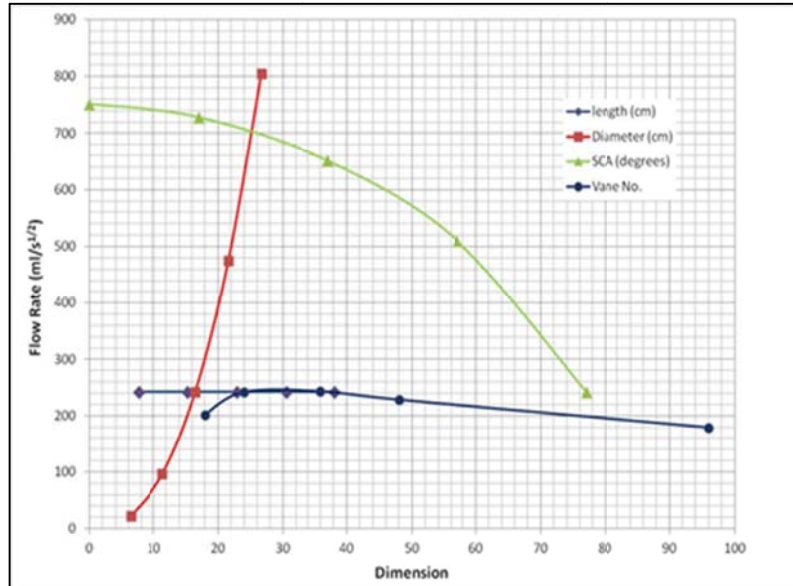


Figure 8. Sensitivity analysis for the compound capillary flow model.

#### IV. Conclusion

It is highly likely that brine dewatering can be conducted in low-g in nearly the same manner as on Earth with capillary forces replacing the role of gravitational forces. Though this work a capillary design has been proposed for a radial vane drying tray or ‘bucket’ which will produce and contain a cylindrical pool of liquid in microgravity. Preliminary analysis and test of the proposed design suggests that the contained liquid pool would be stable against spurious g-disturbances, such as an ISS reboost, and provide sufficient flow rates to support the fill and dewatering processes. Additionally, this work has help refine a set of analytical, numerical, and experimental tools that can be used to quantify the performance of radial vane capillary structures that can be used for brine dewatering and other microgravity fluid management problems, e.g., cryogenic fluids and propellant tanks. These tools will be used in the development of a robust microgravity dewatering system ultimately envisioned to be a lightweight, collapsible, capillary device for recovering water from spacecraft brines and helping to close the water loop for deep space exploration.



## Acknowledgments

The authors gratefully acknowledge Otto Estrada, Dean Muirhead, Chris Carrier, and Letty Vega of the NASA Johnson Space Center Engineering, Technology and Science (JETS) group, and Jason Nelson and Sarah Shull of NASA Johnson Space Center for their contributions, and Mike Flynn and Lance Delzeit, of the NASA Ames Research Center for their contributions, insights, and support as related to BRIC development activities.

## References

- <sup>1</sup>Human Health, Life Support and Habitation Systems Technology Area 06, National Aeronautical Space Administration: April 2012.
- <sup>2</sup>Callahan, M.R., Pensinger, S.J., and Pickering, K.D., "Preliminary Feasibility Testing of the BRIC Brine Water Recovery Concept," AIAA 2012-3526, In *AIAA 42nd International Conference on Environmental Systems*, San Diego, CA, July 2012.
- <sup>3</sup>L.K., Straus, J., and McaCallum, T., "Employing ionomer-based membrane pair technology to extract water from brine," AIAA 2012-3527, In *42nd International Conference on Environmental Systems*, San Diego, CA, July 2012.
- <sup>4</sup>Delzeit, L., Fisher, J.W. "Brine Evaporation Bag Design Concept and Initial Test Results", AIAA 2012-3525, *42nd International Conference on Environmental Systems*, San Diego, CA., July 2012.
- <sup>5</sup>Smith, F., Weaver, G., Lange, K., and Ruemmele, W., "Water Recovery of Reverse Osmosis Brine and Pretreated Urine with an Air Evaporation Subsystem," SAE Technical Paper 1999-01-1992, 1999, doi:10.4271/1999-01-1992.
- <sup>6</sup>Thomas, E., Graf, J., Sweterlitsch, J., Weislogel, M. "Development of the Static Phase Separator", SAE 2008-01-2041, In *38th International Conference on Environmental Systems*, San Francisco, CA, June 2008.
- <sup>7</sup>Weislogel, M. M., Thomas, E. A., and Graf, J. C., "A Novel Device Addressing Design Challenges for Passive Fluid Phase Separations Aboard Spacecraft," *Microgravity Science and Technology*, Vol. 21, 2009, pp. 257-268.
- <sup>8</sup>Concus, P., Finn, R., On the Behavior of a Capillary Free Surface in a Wedge, *Proc. Natl. Acad. Sci. U.S.A.*, 63:2, June 1969, pp. 292-299.
- <sup>9</sup>Weislogel, M.M. Capillary Flow in Interior Corners: the Infinite Corner, *Phys. of Fluids*, 13(11):3101-3107, Nov., 2001.
- <sup>10</sup>McQuillan, J., Pickering, K.D., Anderson, M., Carter, L., Flynn, M., Callahan, M., Vega, L., Allada, R., and Yeh, J. 2010 "Distillation Technology Down-selection for the Exploration Life Support (ELS) Water Recovery Systems Element", AIAA 2012-6125, In *40th International Conference on Environmental Systems*, Barcelona, Spain, July 2010.
- <sup>11</sup>Weislogel, M.M.; Compound Capillary Rise, *J. Fluid Mech.*, Vol. 709, pp. 622-647, (2012).